

Effective crystal field and Fermi surface topology: a comparison of d - and dp -orbital models

N. Parragh¹, G. Sangiovanni¹, P. Hansmann², S. Hummel³, K. Held³, and A. Toschi³

¹*Institut für Theoretische Physik und Astrophysik,
Universität Würzburg, Am Hubland, D-97074 Würzburg, Germany*

²*Centre de Physique Théorique, Ecole Polytechnique,
CNRS-UMR7644, 91128 Palaiseau, Paris, France*

³*Institut für Festkörperphysik, Technische Universität Wien, 1040 Vienna, Austria*

The effective crystal field in multi-orbital correlated materials can be either enhanced or reduced by electronic correlations with crucial consequences for the topology of the Fermi surface and, hence, on the physical properties of these systems. In this respect, recent local density approximation (LDA) plus dynamical mean-field theory (DMFT) studies of Ni-based heterostructure have shown contradicting results, depending on whether the less correlated p -orbitals are included or not. We investigate the origin of this problem and identify the key parameters controlling the Fermi surface properties of these systems. Without the p -orbitals the model is quarter filled, while the d manifold moves rapidly towards half-filling when the p -orbitals are included. This implies that the local Hund's exchange, while rather unimportant for the former case, can play a predominant role in controlling the orbital polarization for the extended basis-set by favoring the formation of a larger local magnetic moment.

PACS numbers: 71.10.-w, 71.27.+a, 73.40.-c

I. INTRODUCTION

Correlated electronic systems display some of the most fascinating phenomena in solid state physics. One of their typical characteristics is a strong sensitivity to small changes of external control parameters. Hence, a precise understanding of the underlying physics and of the pivotal parameters controlling the observed phenomenology represents a crucial goal in contemporary condensed matter research, also in light of possible applications beyond the purely academic context.

The intrinsic complexity of many-body physics prevents an exact ab-initio theoretical description of correlated materials. In fact, even one of the most basic models for electronic correlations, i.e. the Hubbard model¹ where only the local part of the Coulomb interaction is retained, cannot be exactly solved in the relevant cases of two or three dimensions. However, a great step forward in the theoretical analysis of electronic correlation in condensed matter was achieved in the last decades by means of dynamical mean-field theory (DMFT)^{2,3}, and, for realistic material calculations, by its merger with ab-initio density functional approaches (LDA+DMFT)⁴.

From the theoretical point of view, DMFT-based methods can be viewed as a quantum extension of the classical mean-field approaches. Hence, the application of DMFT implies neglecting all non-local spatial correlations albeit allowing for a very accurate (and non-perturbative) treatment of the most relevant part of the electronic correlations stemming from the (single or multi-orbital) Hubbard interaction i.e., their purely local part. The ability of DMFT to capture these local quantum fluctuations is one of the keys behind its success in addressing many open questions in the physics of strongly correlated materials. Among those, we recall

the pioneering DMFT description of the Mott⁵ metal-insulator transition (MIT) in V_2O_3 ^{3,6}, of the δ phase of Pu⁷, of the correlation effects⁸ in Fe and Ni, of the volume collapse in Ce⁹, of the unconventional pairing mechanism of superconductivity in fullerenes¹⁰; most recently DMFT has been also successfully applied to the analysis of the occurrence of kinks in the self-energy¹¹ and in the specific heat¹² of particular vanadates, such as SrVO₃, and LiV₂O₄, as well as of the spectral and magnetic properties^{13,14} of Fe-based superconductors.

Furthermore, it should also be recalled here, that DMFT is a very flexible scheme, whose application is possible also beyond the standard case of bulk correlated systems. In fact, DMFT-based methods have been recently used to study correlated nanoscopic¹⁵ and heterostructures¹⁶⁻¹⁸. For the latter case, we want to focus here, in particular, on the theoretical predictions for the Fermi-surface properties of layered Ni-based heterostructures. The application of LDA+DMFT to this problem, and more specifically, to the case of a 1:1 layered LaNiO₃/LaAlO₃ heterostructure has raised a considerable interest, as the DMFT results of Refs. 18 and 19 clearly prospect the possibility to drive the Fermi surface “topology” of these materials very close to the one of the high-temperature superconducting cuprates. In fact, the electronic structure in the bulk Nickelates, such as R_{1-x}Sr_xNiO₄, is typically characterized by two bands crossing the Fermi level²⁰, which arise from the two e_g -orbitals of Ni (the “planar” $x^2 - y^2$ and “axial” $3z^2 - r^2$ -orbital). However, by growing heterostructures with planes of LaNiO₃ intercalated with insulating planes of LaAlO₃ and on substrates providing an epitaxial strain, such as SrTiO₃ or PrScO₃, the energetic configuration of the $3z^2 - r^2$ will be correspondingly disfavored²¹, which corresponds to a (by our definition positive) crystal field

splitting $\Delta_{CF}^d = \varepsilon_{3z^2-r^2} - \varepsilon_{x^2-y^2} > 0$ among the two Ni e_g -orbitals. In this situation, LDA+DMFT calculations have shown that the inclusion of the correlation effects will always increase the original (LDA) crystal field splitting between the two e_g -orbitals²², leading, eventually, to a significant change of the “topology” of the Fermi surface, i.e. to a situation in which only *one* band, with predominant $x^2 - y^2$ -character crosses the Fermi level. Hence, according to these LDA+DMFT calculations, in Ni-based heterostructures it would be possible to “artificially” realize the electronic configuration of the high-temperature superconducting cuprates (i.e., single, almost half-filled orbital with $x^2 - y^2$ symmetry close the Fermi level), e.g. by modulating the strain through changing the substrate or the insulating layer. As the control of the low-Fermi surface properties represents an essential ingredient for novel, alternative, realizations of high-temperature superconductivity, the importance of having highly accurate LDA+DMFT predictions becomes a crucial factor for engineering new materials.

In contrast to these impressive applications of DMFT-based methods, one important aspect should be stressed here: The LDA+DMFT procedure requires as an important step a downfolding to a chosen energy window around the Fermi energy ε_F . For most of the above mentioned studies, this window included only a few bands around ε_F of dominant 3d character. In such basis for the transition metal oxides the hybridization of 3d states and oxygen ligand 2p states is included *implicitly* in the effective bands. In the recent past, however, it has become customary to include the oxygen 2p states *explicitly*, i.e. to downfold to a larger energy window. In most of the cases, these additional (p -) orbitals were way more extended than the correlated ones (e.g. d), and, hence, the local Coulomb interaction between electrons occupying these additional orbitals (U_{pp}) and between electrons on different manifolds (U_{pd}) was either completely neglected, or, in some exceptional cases, treated at the Hartree level²⁵. Despite this approximation, it is quite intuitive to expect that the validity of LDA+DMFT calculations performed in an enlarged (say: dp) basis-set is more general than the corresponding one in the restricted d manifold. In fact, quite generally: (i) performing a renormalization (Wannier²⁶ projection, NMTO²⁷ downfolding, etc.) on an enlarged basis-set allows for a better localization of the orbitals of the correlated manifold (as the dp -hopping processes are now explicitly included in the model); and (ii) the possibility of describing explicitly charge-transfer processes between the d and p -orbitals makes the theoretical modeling evidently closer to the actual material physics²⁸.

Notwithstanding these quite general arguments, the improvement of LDA+DMFT calculations on enlarged dp basis-sets w.r.t. the ones restricted to effective d -only basis, is not always apparent. In fact, there are cases for which a treatment on a larger basis set renders the comparison with experiment to be worse! Without attempting to give a complete review here, we re-

call that LDA+DMFT calculations including p -orbitals have improved the descriptions of the insulating behavior of NiO²⁹ and of the MIT in NiS₂³⁰ w.r.t. d -only calculations³¹. Also quite accurate results have been obtained for one- and two-particle properties of cobaltates (such as SrCoO₃³² and LaCoO₃³³) and in several studies³⁴ of the well-known class of iron-pnictides and calchogenides.

In contrast to the aforementioned successful applications of dp calculations, in other, equally important, cases the dp LDA+DMFT results are in partial or total contradiction with the d -only calculations, and/or with the experimental findings: No MIT in V₂O₃ was found up to unrealistically large values of the Coulomb interaction if the Oxygen p -orbitals are included in LDA+DMFT calculations³⁵. More recently also the Mott-Hubbard insulating phase of La₂CuO₄ and LaNiO₃ was reported to be missing in the dp framework³⁶, while these materials are found to be insulating in d -only calculations for plausible values of the dd interaction. These discrepancies between d -only and dp calculations regarding the Mott-Hubbard MIT have already raised a discussion in the recent literature. In Ref. 36, non-local correlations to be included beyond DMFT³⁷ have been considered as a cause of the discrepancy. In fact, a major role of spatial correlations in determining the onset of insulating phases is quite likely, especially in the case of two-dimensional cuprates.

However, there are also other discrepancies, whose discussion will be the object of the present work, which can be hardly attributed to the effects of non-local correlations. These discrepancies are observed for systems of more than one correlated d -orbital and in broad parameter regimes (including high temperatures), where effects beyond DMFT should not play a crucial role. In particular, a striking disagreement between d -only and dp calculations was reported for the above-mentioned case of Ni-based heterostructures. In fact, LDA+DMFT calculations performed including also the Oxygen p -orbitals have shown³⁸ exactly the opposite trend w.r.t. the previous ones: Even in presence of a favorable crystal field splitting $\Delta_{CF}^d = \varepsilon_{3z^2-r^2} - \varepsilon_{x^2-y^2} > 0$ at the starting (LDA) level, the net effect of the Hubbard interaction was *always* to reduce the orbital polarization by filling back the $3z^2 - r^2$ -orbital, which would prohibit *de facto* any possibility of realizing the cuprate conditions for the onset of an unconventional superconductivity.

This second kind of discrepancies between LDA+DMFT performed with different (d -only vs. dp) basis-sets well illustrated by the contradicting results for the Ni-based heterostructures, raises a quite general question about the proper use and interpretation of the growing number of LDA+DMFT calculations on extended basis sets. The correct determination of the orbital polarization and Fermi surface properties is of great importance for future calculations of increasingly complex materials.

In this paper we aim at understanding the relations

between the results of existing LDA+DMFT calculations on different basis-sets for the Fermi surface properties of multi-orbital systems and, ultimately, the origin of the qualitative discrepancies observed by following the standard implementation of the algorithms in different basis-sets. For this purpose, it is of primary importance to disentangle the main, qualitative, trends from the specific features of a selected case. Hence, we will study model Hamiltonians for different crystal field splittings starting from a dp -basis (4 bands). Subsequently, we perform a downfolding to an effective d -only basis and compare DMFT results of both cases. This procedure will capture the above-mentioned discrepancy in the prediction of Fermi surfaces of correlated multi-orbital systems and allow for a systematic study of this problem in the context of Ni-based materials.

The scheme of the paper is the following: In Sec. II we introduce the models. In Sec. III, we analyze the disagreement in the calculation of the orbital occupations and the shape of the Fermi surfaces between d -only and dp model for a fixed set of interaction parameters. At the end of Sec. III, we also provide an analysis of the role of Hund's exchange J . In Sec. IV we study the origin of the observed inconsistencies by analyzing the dependence on the d -electron-density, and we discuss its possible relation with the crossover³⁹ from high-spin (Hund's regime) to low-spin (CF regime). Finally, in Sec. V we summarize our results.

II. MODELS AND METHODS

In this section, we illustrate the simplified model Hamiltonians chosen to analyze the discrepancies between the existing LDA+DMFT calculations on different (d -only vs. dp) basis-sets for the prediction of the orbital polarization and the Fermi surface properties of correlated multi-orbital systems. Let us stress that, in this work, we aim at a basic understanding of the general physics underlying the contradicting outcomes of realistic calculations, rather than discussing the case of a specific material. As a guidance for the choice of the model, we recall (see Sec. I) that important inconsistencies in the theoretical predictions emerged already when considering the presumably simple case of two correlated (namely, e_g -)⁴⁰ orbitals only, such as in the case of bulk Nickelates²⁰ and Ni-based heterostructures^{18,19,38}.

Hence, we will introduce here two models (distinguished for the different basis-sets), built with tetragonal symmetry, allowing for the simplest realization of the above-mentioned situation of two correlated orbitals (identified with the two e_g d -orbitals) in the presence of a minimal number of extended ligand orbitals (henceforth associated to p -orbitals). The models are inspired, to some extent, by the realistic calculations of nickelate heterostructures, i.e. with a focus on the orbital polarization in a quasi two-dimensional geometry. However, we will

not consider here spatial correlations beyond DMFT³⁷, the ‘‘dimensionality’’ entering explicitly only via the k -summations defining the local quantities. Therefore, the results will depend mainly on the ‘‘effective’’ crystal field splitting, on the orbital occupation and on the electronic kinetic energies. Furthermore, the general trends emerging from our DMFT calculations are found to be stable w.r.t. the specific parameter choice of the dp and d -only models we are going to consider. Hence, our study will provide useful indications to identify and clarify the global trends of the multi-orbital physics of this class of systems, *at the DMFT level*.

Specifically, the model Hamiltonians considered will be the following:

1. The one-particle model Hamiltonian for the larger basis-set, from which we start conceptually, is a dp four-band model (Fig.1 upper panels), that includes explicitly two correlated d -orbitals (e.g., the Nickel $3d-e_g$ states), and two ligand (e.g., Oxygen $2p$ states).
2. The model for the smaller basis-set is the (Löwdin) downfolded^{41,42} version of the first one on the two correlated (e.g. $3d-e_g$) orbitals: It corresponds to the two-orbital d -only band-structure, shown with the corresponding orbital character in Fig.1 (lower panels).

Note that, due to the downfolding, the band structure of the two models at the Fermi level are identical by construction. Yet the associated orbital character is different.

dp four-band model

While DMFT calculations are often performed first in the smallest possible basis-set, for the definition of our one-particle model Hamiltonians it is conceptually more logical to start from a larger (dp) basis-set. In our case, this includes two correlated d -orbitals and two ligand p -orbitals. The specific dispersion considered corresponds to a quasi two-dimensional geometry of the model, which can be thought of as one p_x - and one p_y -orbital on each ligand site. The overlap between the ligand orbitals and the two e_g orbital gives the largest contribution to the hopping processes (t_{pd}). Hence, for the sake of simplicity, the smaller direct hopping among d -orbitals is neglected ($t_{dd} = 0$). Furthermore, in our one-particle Hamiltonian the d and the p manifold are kept well distinguishable, in that a large enough dp splitting is assumed (see below for details). These choices correspond to the minimal dp model with a realistic dp configuration in a (quasi two dimensional) cubic/tetragonal symmetry.

The specific values of the parameters, e.g., the dp -hopping amplitude (t_{pd}), on-site d/p energies, and crystal field splitting among the d -orbitals (Δ_{CF}) have therefore been chosen to obtain a reasonable bandwidth for

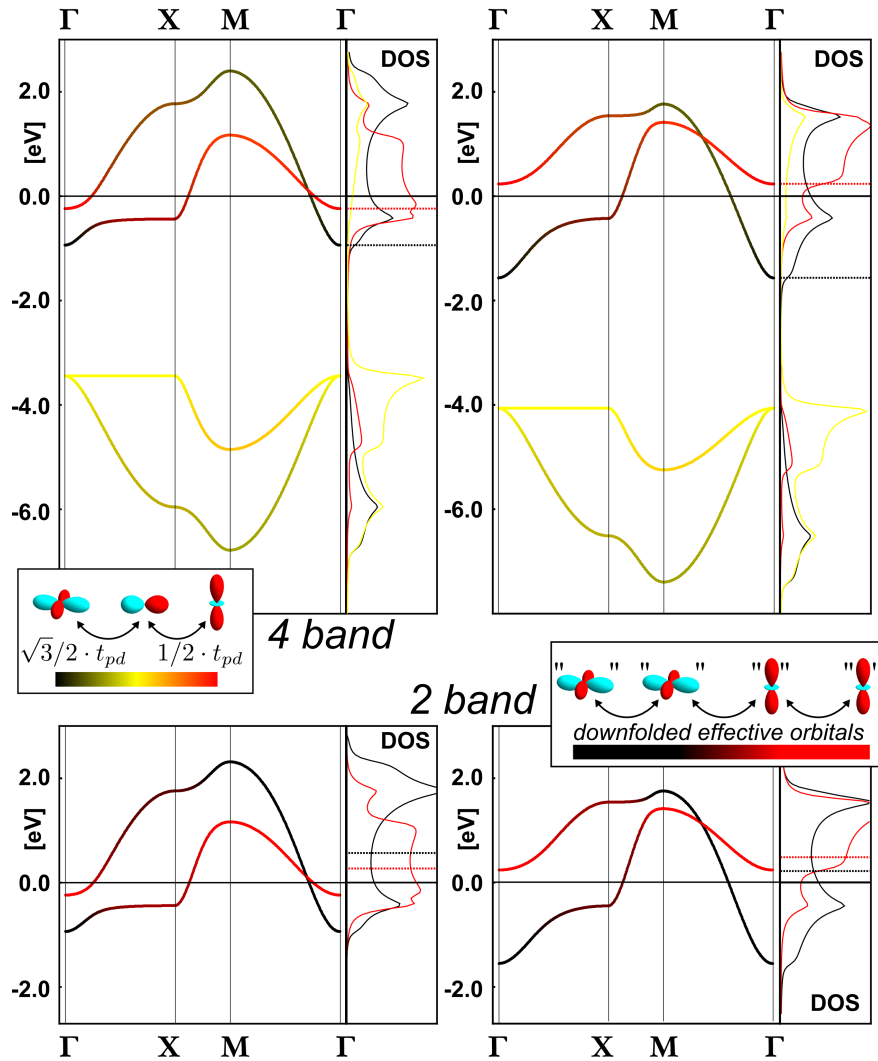


FIG. 1. Band-structure and DOS of the four-band dp model (upper panel) and the corresponding downfolded two-band dp model (lower panel) for two different values of the crystal field splitting Δ_{CF} between the e_g -orbitals of the dp Hamiltonian, Eq. 1. Specifically these are $\Delta_{CF} = 0.7\text{eV}$ (left panels) and 1.7eV (right panels), corresponding to a local energy splitting $\Delta_{CF}^d = -0.53\text{eV}$ and 0.37eV respectively in the d -only model. The orbital character is denoted by the following color-coding: black for the first d -orbital ($x^2 - y^2$), red for the second ($3z^2 - r^2$), and yellow for the p -orbitals. In the inset, the hopping processes for the two models are sketched.

the bands close to the Fermi level. Our choice also ensures that the positive/negative values assumed by the splitting Δ_{CF}^d between the two downfolded d -orbitals in the small basis-set are plausible. This way we build up a one-particle low-energy Hamiltonian similar to the 4-

band cuprate Hamiltonian derived in Ref. 43, whereas the role of our “axial” orbital $3z^2 - r^2$ is played by the $4s$ -orbital of Cu. Formally, our dp Hamiltonian in momentum space reads:

$$H_{\mathbf{k}}^{4b} = \begin{pmatrix} 0 & 0 & i\sqrt{3}t_{pd} \sin\left(\frac{k_x}{2}\right) & -i\sqrt{3}t_{pd} \sin\left(\frac{k_y}{2}\right) \\ 0 & \Delta_{CF} & it_{pd} \sin\left(\frac{k_x}{2}\right) & it_{pd} \sin\left(\frac{k_y}{2}\right) \\ -i\sqrt{3}t_{pd} \sin\left(\frac{k_x}{2}\right) & -it_{pd} \sin\left(\frac{k_x}{2}\right) & \epsilon_p & 0 \\ i\sqrt{3}t_{pd} \sin\left(\frac{k_y}{2}\right) & -it_{pd} \sin\left(\frac{k_y}{2}\right) & 0 & \epsilon_p \end{pmatrix}, \quad (1)$$

where the lattice spacing $a = 1$, $t_{dp} = 1.8\text{eV}$ and $\Delta_{CF} = [0.7, 1.7]\text{eV}$ ($\Delta_{CF}^d = [-0.53, +0.37]\text{eV}$) for the reason explained above. The on-site energy of the p -states was fixed to $\epsilon_p = -2.5\text{eV}$ similar to the position of the p -bands in the nickelate systems. As for the Fermi level, the model is assumed to have typically overall filling of 5 electrons. This would correspond, ideally, to the situation of filled ligand bands and to a quarter-filled correlated two-band manifold at the Fermi level.

In the lower panels of Fig. 1, we show the bandstructure of the four-band dp model corresponding to the two extreme values of Δ_{CF} we considered. In the bandstructure and DOS plots the black/red color encodes the d -character ($x^2-y^2/3z^2-r^2$, respectively), and the yellow color encodes the p -character.

d-only two-band model

The d -only model has been obtained by means of a Löwdin downfolding of the dp Hamiltonian, Eq. 1 which means that their respective electronic structure at the Fermi level is identical by construction. The overall result of the downfolding procedure is reported in the corresponding orbitally-resolved bandstructure for the two-band model in Fig. 1 (bottom panels). Specifically, the bandstructure and DOS of Fig. 1 have been obtained by downfolding the dp Hamiltonians with the lowest and the highest value of Δ_{CF} (and Δ_{CF}^d), respectively. The orbital occupation of the d -only model has been fixed to $n_d = 1$ (quarter-filling).

In Fig. 1 the color code denotes, similarly as before, the orbital character: black and red represent the downfolded x^2-y^2 - and $3z^2-r^2$ -orbital, respectively. At a closer inspection of the figure, we note that, while locally the two e_g -orbitals are eigenstates of the tetragonal point group and do not hybridize (pure black/red color of the DOS), they do obviously hybridize non-locally along certain directions (dark-red color, e.g. at the X point of the Brillouin zone). Furthermore, we observe that the overall width (as well as the associated kinetic energy) of the $3z^2-r^2$ DOS is smaller than the x^2-y^2 one, a typical feature of anisotropic materials and/or heterostructures with a quasi two-dimensional hopping geometry with suppressed hopping along the c -axis. More importantly for our purposes, we stress how the different original values of Δ_{CF} in the dp basis-sets correspond to situations with negative/positive difference between the center of mass of the non-interacting DOS of our d -only model. Specifically, this means that the important

parameter $\Delta_{CF}^d = \epsilon_{3z^2-r^2} - \epsilon_{x^2-y^2}$, accounting for the on-site energy difference⁴⁵ between the two e_g states in the downfolded model, will be varying in the range of $[-0.53, 0.37]$ depending on the chosen value of Δ_{CF} in the starting dp Hamiltonian. We stress here, that Δ_{CF}^d can be interpreted, to a certain extent, as “crystal field” within the d -only manifold. However, by adopting such a “rough” definition, one should keep in mind that Δ_{CF}^d is, in fact, a “ligand field” splitting, originated by an electrostatic Madelung potential and a dp -hybridization splitting.

Before discussing some technical aspects of our DMFT implementation in the next subsection, we recall that related two-band model Hamiltonians, but *without* hybridization between the d -orbitals, have been studied with DMFT in Ref. 39, with reference to the cases of BaVS₃ and Na_xCoO₂.

DMFT algorithm in extended basis-sets

The DMFT algorithm applied to a chosen correlated orbital-subspace, possibly derived from ab-initio calculations, has already become a quite standardized procedure (for details we refer the reader to 4). However, in consideration of the discrepancies appearing when extending the basis-set by including less-correlated ligand p -orbitals in the self-consistent DMFT loop, we will explicitly recall here some technical aspects of the DMFT algorithmic procedure usually adopted in the cases of the extended dp -basis-sets.

Extended models including ligand p -states explicitly have a structure like our 4-band Hamiltonian (1). Locally, i.e. integrated over the Brillouin zone, such Hamiltonian has the form:

$$H_{\text{full}}^{\text{loc.}}(R=0) = \begin{pmatrix} H_{dd}^{\text{loc.}} & H_{dp}^{\text{hyb.}} \\ (H_{dp}^{\text{hyb.}})^\dagger & H_{pp}^{\text{loc.}} \end{pmatrix} \quad (2)$$

The local basis is typically chosen in a way that the H_{dd} and H_{pp} blocks can be made internally diagonal after \mathbf{k} -integration so that the states can be labeled by a good *local* quantum number in the respective subspaces, such as the crystal field labels (see DOS plots in Fig. 1). In such a basis, the local Coulomb (U) matrix of the interacting part of the Hamiltonian is then defined (in its SU(2)-invariant “Kanamori”) form as

$$H_{\text{loc}} = \sum_a U n_{a,\uparrow} n_{a,\downarrow} + \sum_{a>b,\sigma} [U' n_{a,\sigma} n_{b,-\sigma} + (U' - J) n_{a,\sigma} n_{b,\sigma}] - \sum_{a \neq b} J (d_{a,\downarrow}^\dagger d_{b,\uparrow}^\dagger d_{b,\downarrow} d_{a,\uparrow} + d_{b,\uparrow}^\dagger d_{b,\downarrow}^\dagger d_{a,\uparrow} d_{a,\downarrow} + h.c.).$$

for the d -orbital sector. Here, U denotes the interaction parameter between two electrons in the same d -orbital, U' the interaction between electrons on different d -orbitals and J is the Hund's coupling; a, b index the two orbitals and σ the spin. Note that the specific interaction values for the DMFT calculations (see next section for details) have been chosen in order to reproduce a typical correlated metallic situation. Due to the stronger localization of the d -orbitals in the dp models, the corresponding values of the local interaction on the d -orbitals have been correspondingly enhanced (we assumed here a factor two for the parameter U'). We recall that – for the dp case – the multi-orbital Hubbard interaction could include, besides on-site d and on-site p interactions, also possible dp interactions. This is, however, not the topic of the present study. Furthermore, for the dp model in LDA+DMFT we have to face the so-called problem of *double-counting correction* (DC)^{4,46,47}: Unlike for a d -only model, this does not correspond to a simple total energy shift and, hence, cannot be “absorbed” in the chemical potential. The DC for the dp models corresponds to a renormalization of the energy difference between d and p states. For our models we have used the DC suggested by Anisimov⁴⁶, given by:

$$\begin{aligned}\bar{U}_{dd} &= [U + U'(N_d - 1) + (U' - J)(N_d - 1)] / (2N_d - 1) \\ \Delta_{DC} &= \bar{U}_{dd}(\sum_d n_d^{LDA} - \frac{1}{2}),\end{aligned}\quad (3)$$

where N_d is the number of d -orbitals, and \bar{U}_{dd} is the average local interaction between these d -orbitals; n_d^{LDA} denotes the occupation of the d -orbitals as calculated from the \mathbf{k} -resolved non-interacting (LDA) Hamiltonian discussed above.

The self-consistent DMFT loop, which includes the solution of an Anderson impurity problem for the correlated subspace at each step is done as follows:

1. The first step is the calculation of the \mathbf{k} -integrated Green function on the *full* dp basis-set:

$$G_{\text{full}}^{\text{loc.}}(\omega) = \frac{1}{V_{\text{BZ}}} \int_{\text{BZ}} d^3k \quad [(\omega + \mu)\mathbb{1} - H_{\mathbf{k}}^{4b} - \Sigma_{\text{full}}(\omega)]^{-1} \quad (4)$$

where G , Σ_{full} , and $H_{\mathbf{k}}$ are matrices in the dp -basis.

2. Next, we extract the dd -block of the local Green function:

$$G_{dd}^{\text{loc.}}(\omega) = \{G_{\text{full}}^{\text{loc.}}(\omega)\}_{|dd\text{-block}}, \quad (5)$$

i.e. we project it onto the d -subspace. We stress here, that due to the dp hybridization encoded in the Hamiltonian $H_{\mathbf{k}}^{4b}$ and the inversion of Eq. 4 the information about the p -ligands is not lost but captured by $G_{dd}^{\text{loc.}}(\omega)$.

3. Now, in complete analogy to DMFT for d -states only, we calculate the Weiss field for the impurity model (only on the d -subspace):

$$[\mathcal{G}^0(\omega)]^{-1} = [G_{dd}(\omega)]^{-1} + \Sigma_{dd}^{\text{DMFT}}(\omega), \quad (6)$$

where $\Sigma_{dd}^{\text{DMFT}}(\omega)$ denotes the DMFT dd self-energy.

4. With $\mathcal{G}^0(\omega)$ we solve the auxiliary impurity problem (see below), obtain a new impurity Green function and a new self-energy for the d -orbitals. Finally the self-consistent loop is closed by comparing both the new and the old $\Sigma_{dd}^{\text{DMFT}}(\omega)$ and the new and the old d/dp -density and iterating until convergence.

As impurity solver for our DMFT calculations, we have used the continuous time quantum Monte-Carlo (QMC) algorithm in the hybridization expansion (CT-HYB)^{48,49}, which allows also for the treatment of the spin-flip and pair-hopping terms of our Kanamori Hamiltonian (3). In the CT-HYB the time evolution is calculated using the local interaction, which makes the local Hilbert space growing exponentially with the number of orbitals. While for density-density interactions this problem can be mitigated along the line of^{48,50}, for the more realistic Kanamori interaction a set of quantum numbers, called PS, leads to a more efficient algorithm⁵¹. We have used this to perform all calculations presented in this paper with the full SU(2)-symmetric Hamiltonian.

III. RESULTS: d VS dp CALCULATIONS AT “QUARTER-FILLING”

In this section, we compare our DMFT results obtained in the two different basis-sets. Following the chronological order of appearance of realistic LDA+DMFT calculations for these systems, we present data for the d -only (downfolded) basis-set first and then the corresponding ones for the original dp Hamiltonian.

We mention that our model study can be qualitatively related, depending on the initial value of the energy splitting between the correlated orbitals ($\Delta_{CF}^d = \varepsilon_{3z^2-r^2} - \varepsilon_{x^2-y^2}$), to the physics of bulk Nickelates²⁰ and of Ni-bases heterostructures^{18,19,38}. In fact, (i) the nominal charge of these systems corresponds also to one electron in the outer two Ni-bands and (ii) the bulk Nickelates are typically characterized by negative values of Δ_{CF}^d , due to the tetragonal distortion along the z -axis. In the Ni-based heterostructures instead, the localization effects in the z direction, as well as the epitaxial strain due to the substrate, induce positive values for Δ_{CF}^d .

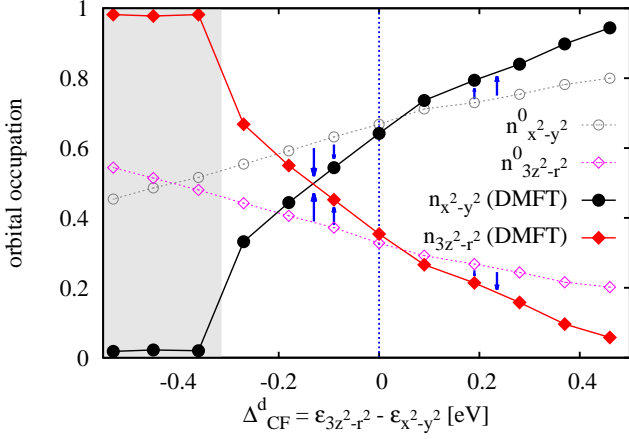


FIG. 2. Orbital occupation of the d -only model with $U' = 4\text{eV}$, $J = 0.75\text{eV}$ ($U = 5.5\text{eV}$), $\beta = 100\text{eV}^{-1}$ at quarter-filling ($n_d = 1$) as a function of the initial crystal field splitting Δ_{CF}^d . The DMFT data (solid symbols) are compared with the corresponding non-interacting results (empty symbols). The arrows indicate the effect of the interaction which is essentially opposite for negative and positive Δ_{CF}^d . The shaded region on the left indicates the onset of the Mott-Hubbard insulating phase.

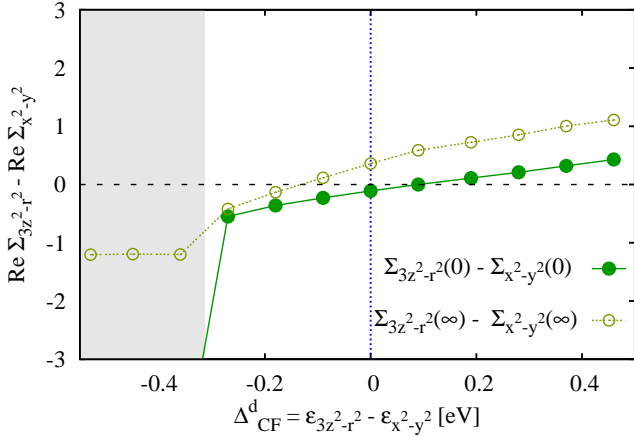


FIG. 3. Difference of the real part of the DMFT self-energies for the two orbitals of the d -only model with $U' = 4\text{eV}$, $J = 0.75\text{eV}$ ($U = 5.5\text{eV}$), $\beta = 100\text{eV}^{-1}$ at quarter-filling ($n_d = 1$) extrapolated to $\omega_n \rightarrow 0$ (solid symbols) and $\omega_n \rightarrow +\infty$ (empty symbol, Hartree contribution to the self-energy) as a function of the initial energy splitting Δ_{CF}^d . The huge enhancement of the difference between the self-energy at $\omega_n \rightarrow 0$, and the consequent huge energy shift of the first orbital, marks the onset of the Mott-Hubbard insulating phase (shaded region on the left).

A. DMFT results for the (downfolded) d -only model

In this subsection, we analyze the results for our d -only two-orbital model at quarter-filling ($n_d = 1$), as a function of the initial energy splitting between the two downfolded e_g -orbitals (Δ_{CF}^d): the corresponding results for the orbital occupation without interaction (which would correspond to the LDA ones, in a realistic calculation) and with the interaction (computed with DMFT) are shown in Fig. 2. As mentioned in Sec. II, the interaction values have been chosen in consideration of typical values for transition metal oxides systems: for the d -only model, we adopted a value of $U' = U - 2J = 4\text{eV}$, with $J = 0.75\text{eV}$ ($U = 5.5\text{eV}$).

We start by briefly commenting the set of non-interacting data shown in Fig. 2: They display a clear-cut dependence on the initial value of the energy splitting of the e_g -orbitals: the orbital occupation of the $x^2 - y^2$ monotonously increases upon increasing values of Δ_{CF}^d , whereas the occupation of the $3z^2 - r^2$ -orbital decreases. We note, however, that, since the hopping terms (and, hence, the bandwidth) for the two orbitals are not equal, the orbital occupation curves are not symmetric w.r.t. to Δ_{CF}^d . This also implies that the situation where the two orbitals are equally occupied (i.e. no orbital polarization) does not occur at $\Delta_{CF}^d = 0$ but, for the non-interacting case, only for $\Delta_{CF}^d \sim -0.4\text{eV}$.

We discuss now the effects of the Hubbard interaction on the orbital occupations, as described by our DMFT(CT-QMC) calculations. While the occupation curves remain obviously asymmetric also in presence of the interactions, from the data of Fig. 2 we note that, for each orbital, the deviations w.r.t. to the non-interacting values are strongly dependent on Δ_{CF}^d : The sign of the change in the orbital occupations appears closely connected with the sign of Δ_{CF}^d . Specifically, for $\Delta_{CF}^d > 0$ we observe generally an enhancement (reduction) of the occupation of the first(second), $x^2 - y^2$ - ($3z^2 - r^2$ -) orbital, while for $\Delta_{CF}^d < 0$ the trend is the opposite.

This is reflected in an analogous trend of the change to the orbital polarization P , formally defined as in Refs. 38 and 52

$$P = \frac{n_{x^2-y^2} - n_{3z^2-r^2}}{n_{x^2-y^2} + n_{3z^2-r^2}}. \quad (7)$$

as well as in the Fermi surfaces, shown in Fig. 6. For the latter ones, which will be discussed more extensively in the next-subsection, our DMFT results show that, depending on the sign of the initial orbital splitting (Δ_{CF}^d), the character (as well as the typical shape) of the Fermi surface corresponding to the lower-energy orbital gets increased by the electronic interaction.

In fact, such trends explain the qualitatively different LDA+DMFT results previously obtained for the shape of the Fermi surface via specific d -only calculations for bulk nickelates²⁰ and Ni-based heterostructures^{18,19}, respectively: The difference in the results essentially re-

flects the different sign of the initial crystal field splitting (Δ_{CF}^d), as estimated by the ab-initio calculations, whose final size (Δ_{eff}^d) gets significantly magnified by the electronic interaction.

The last statement can be formalized more quantitatively through the analysis of the corresponding self-energies presented in Fig. 3: here we show the differences between the real parts of the DMFT self-energy of the two orbitals, i.e. $\text{Re}\Sigma_{3z^2-r^2}(i\omega_n) - \text{Re}\Sigma_{x^2-y^2}(i\omega_n)$, evaluated in the limit frequency $\omega_n \rightarrow 0$ and $\omega_n \rightarrow +\infty$, respectively. We recall that in the latter limit only the Hartree contributions to the electronic self-energy remain. Hence, the difference between the self-energies can be also explicitly written in terms of the electronic density as:

$$\begin{aligned} \text{Re}\Sigma_{3z^2-r^2}(\infty) - \text{Re}\Sigma_{x^2-y^2}(\infty) &= (U - 5J) \times & (8) \\ (n_{x^2-y^2} - n_{3z^2-r^2}) &= (U - 5J) P. \end{aligned}$$

Here, the last equality only holds at quarter-filling where $n_{x^2-y^2} + n_{3z^2-r^2} = 1$. Such a dependence on the (final) electronic density appears evidently in the corresponding data of Fig. 3. The Hartree contribution, evaluated in DMFT, changes sign⁵³ precisely where the orbital occupations become equal ($P = 0$), i.e. for the negative values of $\Delta_{CF}^d \sim -0.15$ eV, see Fig. 2. By comparing this to the previous results, it appears that the high-frequency values of the self-energy do not represent the ‘‘crucial’’ parameter. Instead, the trends in the orbital polarization and, therefore, the predicted physics are controlled by the low-frequency behavior of the self-energy: Up to the MIT the shape of the Fermi surface is determined by the ‘‘effective’’ CF splitting given by

$$\Delta_{eff}^d = \Delta_{CF}^d + \text{Re}\Sigma_{3z^2-r^2}(0) - \text{Re}\Sigma_{x^2-y^2}(0), \quad (9)$$

i.e. as the original crystal field corrected by the difference of the real self-energies for $\omega_n \rightarrow 0$. This makes the interpretation of the second set of data shown in Fig. 3 very transparent: the sign of $\text{Re}\Sigma_{3z^2-r^2}(0) - \text{Re}\Sigma_{x^2-y^2}(0)$ follows that of the original crystal field Δ_{CF}^d , and confirms, from the microscopic point of view, the picture of interaction effects *always* magnifying the size of the original crystal field. Of course such enhancement will depend quantitatively on many factors: For instance, it will be bigger when the system is more correlated. A dramatic enhancement, in particular, is found when the Mott metal-insulator transition is approached, i.e. when Δ_{CF}^d approaches the shaded area in Fig. 3. Here the low energy physics correspond to an empty (broader) x^2-y^2 -orbital and a half-filled (narrower) $3z^2-r^2$ -orbital.

However, as we will now discuss, these results are contradicted by corresponding calculations performed in larger basis-sets, which include also the most relevant p degrees of freedom, as it will be shown explicitly in the next subsection.

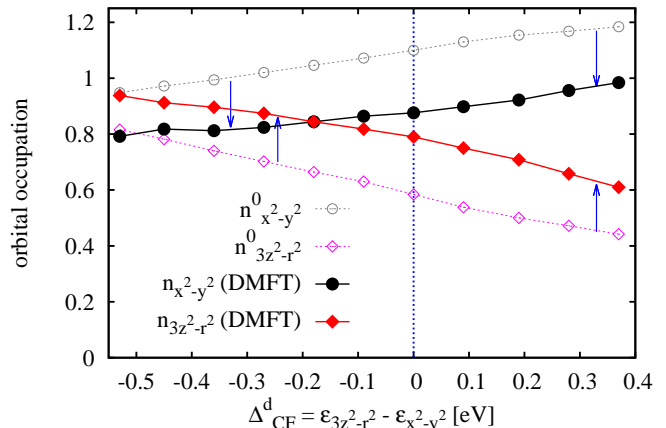


FIG. 4. Orbital occupation of the d -orbitals as a function of the initial crystal field splitting for the four-band dp model with $U' = 8\text{eV}$, $J = 1.0\text{eV}$ ($U = 10\text{eV}$), $\beta = 100\text{eV}^{-1}$ and $n_{tot} = 5$. The DMFT data (solid symbols) are compared with the corresponding non-interacting results (empty symbols).

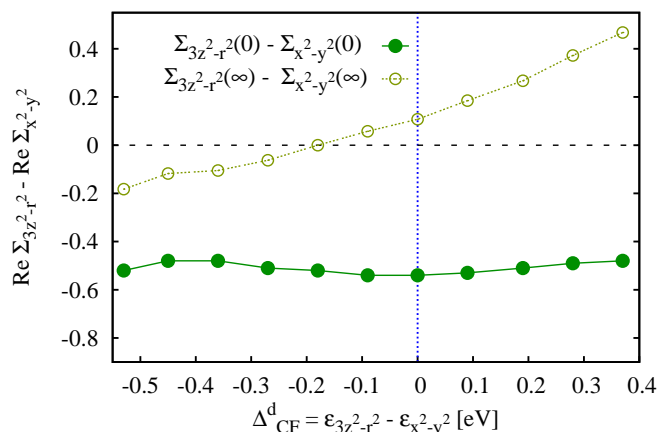


FIG. 5. Difference of the real part of the DMFT self-energies for the two d -orbitals of the four-band dp model with $U' = 8\text{eV}$, $J = 1\text{eV}$ ($U = 10\text{eV}$), $\beta = 100\text{eV}^{-1}$ and the filling is $n_{tot} = 5$. Shown is the low and high frequency asymptotes, i.e. the extrapolation to $\omega_n \rightarrow 0$ (solid symbols) and $\omega_n \rightarrow +\infty$ (empty symbol, Hartree contribution to the self-energy).

B. DMFT results for the dp model

For the 4 band dp model the total occupation is $n_{tot} = n_p + n_d = 5$. Because of the stronger localization of the d -orbitals in the dp case, larger values for U , U' and J have been considered: We have doubled the value of U' w.r.t. the calculation discussed in the previous section, i.e. $U' = 8\text{eV}$ ⁵⁴. Because of the smaller screening effects on the Hund’s exchange constant, we have considered a reduced enhancement of J , which has been fixed to 1eV . As before, the relation $U = U' - 2J$ holds.

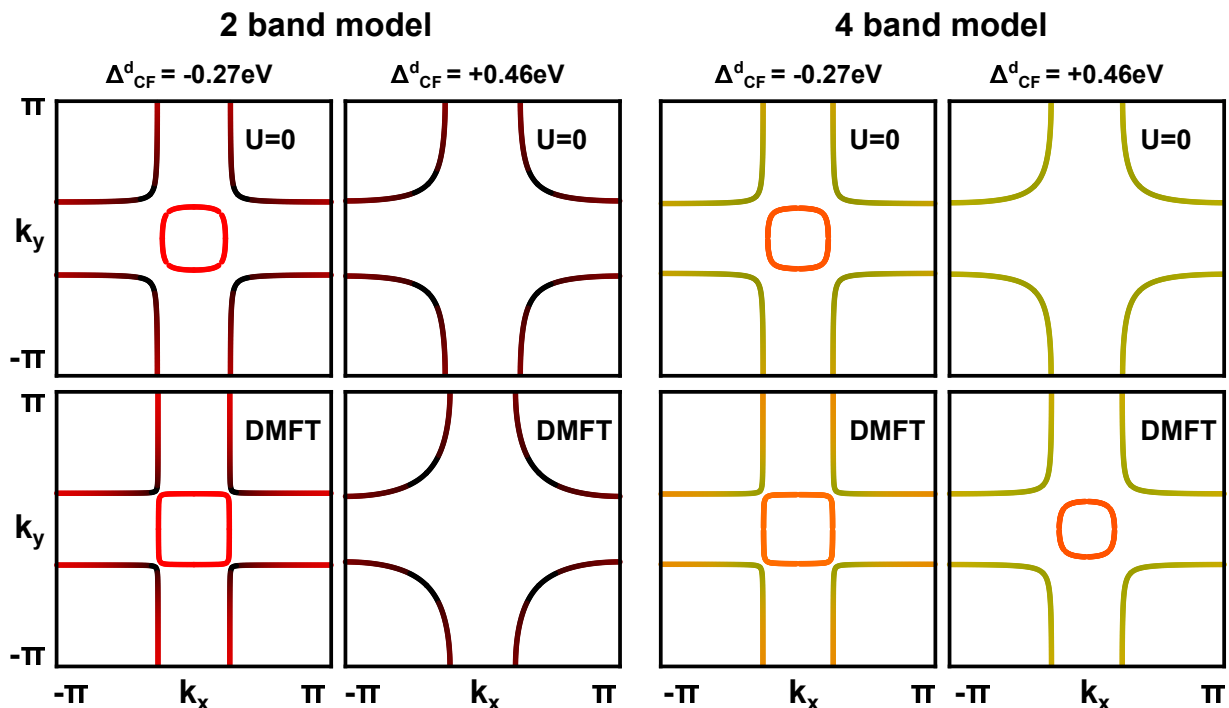


FIG. 6. Shape and orbital character of the electronic Fermi surfaces in the two-different basis-sets (left: d -only model; right: dp model). The DMFT results are shown in the upper and the noninteracting case in the lower row for comparison. The two negative/positive values of Δ_{CF}^d considered, have been chosen as different as possible, with the requirement that a metallic Fermi surface is still found in the interacting case. The color coding of the orbital character (black: $x^2 - y^2$ -, red: $3z^2 - r^2$ -, yellow: p -orbital(s)), is the same as in Fig. 1).

In Fig. 4 we consider first the occupation of the two d -orbitals as a function of the initial crystal field splitting, starting from the non-interacting case. Let us recall here that, because of the downfolding procedure, the numerical values of the energy splitting between the e_g -orbitals in the one-particle Hamiltonian are evidently different in the dp and in the d -only basis-set. They have been labelled, respectively, with Δ_{CF} , see Eq. 1, and Δ_{CF}^d . Note that the latter includes, as *ligand* field, the effects of dp hybridization. To allow for a direct comparison to the effective d -only results we have used the relation between Δ_{CF} and Δ_{CF}^d and plot the dp -results as a function of Δ_{CF}^d .

By analyzing the orbital occupation shown in Fig. 4, the qualitative behavior as a function of Δ_{CF}^d appears similar as in the d -only case. However, an important difference should be noted: In spite of the relatively large separation ($\sim 2\text{eV}$) between d - and p -bands, the total occupation of the d -orbitals is now much larger than before ($n_d \sim 1.7 \div 1.8$) due to the dp hybridization. Quite remarkably, according to our DMFT results of Fig. 4, such an enhanced occupation of the “correlated” d -orbitals essentially survives also upon switching on the local interaction. This fact has an obvious impact on the final results for the orbital polarization P , as now the sign of its change w.r.t. the non-interacting case is no longer related to Δ_{CF}^d : Fig. 4 shows that independently on the

sign Δ_{CF}^d , one *always* observes a reduction of the value of P , i.e. a net enhancement (reduction) of the occupation of the $3z^2 - r^2$ - ($x^2 - y^2$ -) orbital driven by the electronic interaction.

The analysis of the corresponding self-energies provides a further confirmation: Fig. 5 shows the plot of the zero frequency extrapolation of the real part of the self-energy (compare to 3). In contrast to the d -only results now the interaction correction always reduces the initial crystal field, in agreement with the systematic depletion of the $x^2 - y^2$ -orbital (reduction of P) observed in the whole parameter range considered.

On the basis of these results, it is interesting to examine the consequences for the shape of the Fermi surfaces (FS) in the different cases. In Fig. 6 we show the Fermi surfaces for two different values of Δ_{CF}^d for both the d -only and the dp basis-sets. In the upper row we show the non-interacting result and in the lower row the DMFT one. In particular, the two values of Δ_{CF}^d have been chosen to present the extreme cases within our data range (provided that the solution is metallic and has a FS). As for the analysis of Fig. 6, we start by considering the non-interacting FS of the upper row for the two different basis-sets: as a consequence of the Löwdin downfolding, the shape of non-interacting FS corresponding to the same values of Δ_{CF}^d coincide, while the orbital character encoded by the colors differs in that the p contribution is

explicitly present in the dp case. Additionally, for each case considered, the contribution to the FS of the $3z^2-r^2$ -orbital (encoded by the red color and responsible for the formation of the “cylindric”-shaped FS sheet around the Γ -point) is stronger for negative values of Δ_{CF}^d than for positive.

By looking at the DMFT data (lower row) for the dp 4-band model, we see that the overall negative correction to Δ_{eff}^d reported in Fig. 5 gives a definite trend for the Fermi surfaces: In the dp case, the interaction, *independently* of the sign of Δ_{CF}^d always enhances the $3z^2-r^2$ contribution. This is reflected both in the orbital composition (the interacting FS contain more red) and in the shape (enlargement of the central FS sheet). At the same time, our DMFT data unveil quite different trends for the interacting FS of the d -only model: The $3z^2-r^2$ contribution is enhanced *only* for $\Delta_{CF}^d < 0$, i.e., only if the $3z^2-r^2$ was from the beginning the lowest lying of the e_g -orbitals. In fact, coherently with the behavior of Δ_{eff}^d (see Fig. 3), for positive values of Δ_{CF}^d , the interaction further reduces the $3z^2-r^2$ contribution to the FS, which becomes progressively “darker” colored and more “ x^2-y^2 ”-shaped. Let us note that, depending on the details of the dispersion of the specific d -only problem, there are cases in which, for $\Delta_{CF}^d > 0$ the non-interacting FS still presents two-sheets, but the reduction of the $3z^2-r^2$ -character predicted by DMFT, determines a transition to a single sheet FS in the interacting case, analogous to the one calculated in Ref. 18.

Summarizing the main outcome of the comparison of our DMFT calculations in different basis-sets for orbital occupations, crystal field corrections and Fermi surface evolution, an evident *qualitative* disagreement is observed, at least in the region of positive values of the initial crystal field Δ_{CF}^d . It is worth noticing that for positive values of Δ_{CF}^d , the trend we found in the dp -basis-set is consistent with the results of the dp calculations for the Ni-based heterostructures of Ref. 38: There, it was shown, that even when starting from a relatively significant orbital polarization for the x^2-y^2 -orbital at the LDA level, the polarization was always strongly reduced by the interaction, which obviously has bad implications on the possibility of actually manipulating the Fermi surfaces of the Ni-based heterostructures in the “desired” cuprate-like way^{18,21}. As a matter of fact, this discrepancy between d -only and dp results has been found here by also including the SU(2) symmetry of the local interaction on the e_g -bands in both DMFT calculations. This confirms the hypothesis of Ref. 38 that such a discrepancy in the theoretical predictions does not originate from a different treatment of the interactions between the calculations of Refs. 18 and 19 and³⁸, but rather from some more intrinsic difference in the calculations. The most evident systematic difference is the filling n_d of the two e_g -orbitals, which, due to the dp hybridization is strongly increased w.r.t. the quarter-filling level of the d -only model. While this is rather obvious at the LDA level, we note that the occupation of the d manifold does not change much even

in presence of the interaction, for typical choices of the double-counting term for the DMFT (see Sec. II, for details, and also Ref. 38). Quite interestingly, the possible role of an enhanced d -orbital occupation in dp calculations has been also recently addressed, for the different problem of the occurrence of the MIT³⁶.

The point we make here is that the Hund’s exchange J has a strikingly different effect in the d -only and in the dp models, due to the fact that, close to half-filling, J drives the system very effectively towards the Hund’s rule high-spin ground state⁵⁸. For the orbital polarization this means that J does not play a decisive role for the quarter-filled d -only model while it becomes extremely important in the dp model, where $n_d \sim 1.7 \div 1.8$. The d and dp results can indeed be reconciled qualitatively if the Hund’s coupling J for the dp model is equal to $\approx 0.5\text{eV}$ or smaller. This is shown in Fig. 7, in which the dp calculations have been performed reducing the value of J from 1.0eV to $J = 0.5\text{eV}$, and $J = 0.0\text{eV}$ ($U' = U - 2J = 8\text{eV}$ is kept fixed, instead).

The combined analysis of the orbital occupation and of the self-energy (at $\omega_n \rightarrow 0$) results shows that the dp results of Fig 4 and 5 change qualitatively already for the case $J = 0.5\text{eV}$: the overall trend of strong reduction of occupation of the first x^2-y^2 -orbital disappears for a large region of values of the initial crystal field Δ_{CF}^d . In fact, the results already at $J=0.5\text{eV}$ would lead to a physical situation which is qualitatively similar to that predicted by the d -only model. As one can expect, the change with respect to the previous dp results becomes even larger when setting $J = 0.0\text{eV}$, as both trends of orbital occupation and effective crystal field become exactly opposite, with the x^2-y^2 -orbital occupation always increased by the interaction irrespectively of the value of the initial Δ_{CF}^d . The sensitivity of the final dp results on the Hund’s coupling is very illustrative and shows the crucial role of the Hund’s exchange in this situation⁵⁵.

IV. RESULTS: THE ROLE OF THE d -ORBITAL OCCUPATION

From the marked discrepancy between dp and d results, discussed in the previous section, a general question naturally arises: Under which conditions can one expect to obtain a qualitatively similar DMFT description of the interaction effects for d -only and dp calculations?

Let us assume here that we have a very accurate estimate⁵⁹ of the local interactions and especially of the Hund’s exchange J . One of the most basic differences between the d -only and the dp calculations examined is the different value of the occupation of the d -orbitals. This difference is observed already at the level of the non-interacting model and is, remarkably, not strongly affected by the inclusion of the interaction: For the d -only model, the DMFT calculations have been performed, as usual, at fixed filling, while the value of d -orbital occupation for the dp calculations presents moderate oscillations

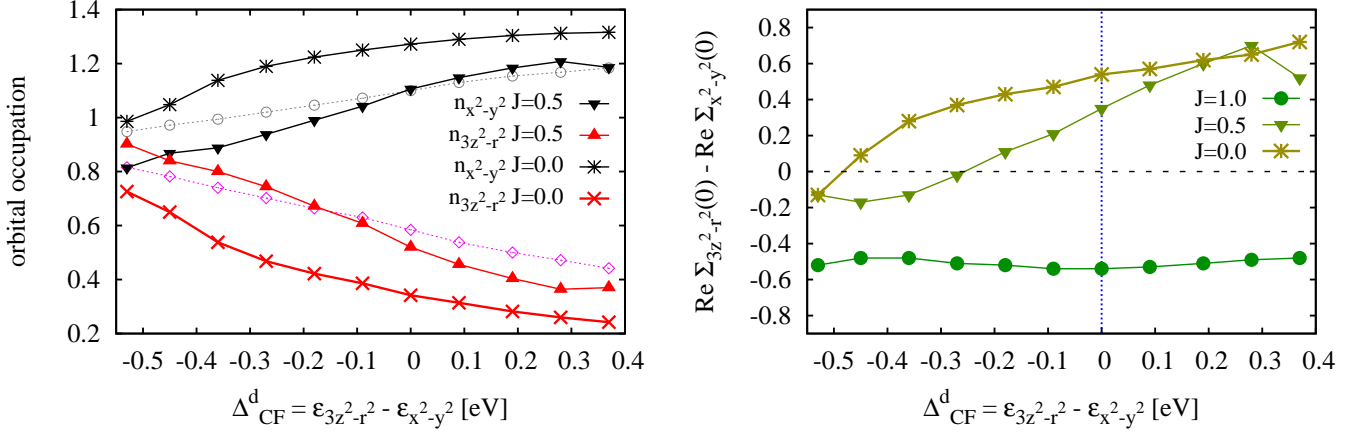


FIG. 7. Left panel: Orbital occupation of the d -orbitals of the four-band dp model as a function of the initial crystal field splitting Δ_{CF}^d . We used $U' = 8\text{eV}$, $\beta = 100\text{eV}^{-1}$, $n_{tot} = 5$ and two different values of the Hund's exchange $J = 0.0, 0.5\text{eV}$. The DMFT data (solid symbols) are compared with the corresponding non-interacting results (empty symbols). Right panel: Corresponding data for the difference of the real part of the DMFT self-energies for the two d -orbitals of the four-band dp model extrapolated to $\omega_n \rightarrow 0$ as a function of the initial crystal field splitting Δ_{CF}^d . The self-energy data are also compared with the corresponding DMFT data at $J = 1.0$, previously shown in Fig. 5.

around a much larger value of $n_d \sim 1.75$, quite independently of the parameter set (U, J, Δ_{CF}^d) considered. Since the filling of the *correlated* orbitals is a crucial factor to drive the system towards a Mott-Hubbard MIT, this will naturally represent one of the key parameters to be considered when comparing LDA+DMFT calculations on different basis-sets.

To make our statement more quantitative, we have performed several additional DMFT calculations for the same d -only model as in Sec. II, but now varying systematically n_d from the original quarter-filling level up to the much higher $n_d \sim 1.75$ found in the dp calculations. The results for the orbital occupations and the self-energy at the Fermi level are shown in Fig. 8 in the upper and lower-row panels, respectively. By gradually increasing the total occupation of the d -orbitals, and focusing on the most interesting regime of $\Delta_{CF}^d > 0$, one observes that the parameter region where the crystal field “drives” the final result (i.e. where its magnitude is enhanced by the interaction), shrinks, being confined to higher and higher values of the initial Δ_{CF}^d .

Looking at the self-energy plot for $n_d = 1.05$, a qualitative change in the trend of the effective crystal field w.r.t. the non-interacting one is found for $\Delta_*^d \sim 0.2$. For $\Delta_{CF}^d < \Delta_*^d$ the trend for the effective crystal field is *opposite* to that observed for quarter-filling, i.e. the original crystal field Δ_{CF}^d is *reduced* by the interaction. An analogous trend is also observed for the changes in the orbital occupations, w.r.t. the non-interacting ones.

By further increasing n_d to 1.25 (second panels of Fig. 8), the threshold Δ_*^d is already shifted beyond the border of the parameter region considered ($\Delta_*^d > 0.5$). Finally, if one performs the DMFT d -only calculations for $n_d = 1.75$, which is roughly similar as in dp model, one

indeed finds a similar behavior as for the dp model: the interaction correction to the crystal field (Fig. 8), overall negative for all positive values of Δ_{CF}^d considered, resembles that of the dp model in Figs. 5, reflecting the tendency to deplete the $x^2 - y^2$ -orbital in presence of the electronic interaction.

For a more general analysis of our data in the whole range of Δ_{CF}^d , let us first recall that, due to the different bandwidths of the two e_g -orbitals, no symmetric behavior between the regions of positive and negative Δ_{CF}^d can be expected. In particular, in the region $\Delta_{CF}^d < 0$ (i.e., the less relevant one in the perspective of the Ni-based heterostructures), the crystal field “enhancement” at quarter-filling was much larger than the corresponding one for $\Delta_{CF}^d > 0$ (see Fig. 3), also as an effect of the closer proximity of the MIT in this parameter region. Hence, while the effects of an increased n_d are always at work, here they become first visible as a gradual weakening of the quarter-filling trends (e.g., as a mitigation of the strongly negative correction to the effective crystal field for $\Delta_{CF}^d < 0$), before getting to an inversion of them: The gray shadow area, marking the onset of the MIT for one of the two orbitals i.e., the (almost) half-filled one, is shrinking in the $n_d = 1.05$ plot, and essentially disappears at $n_d = 1.25$. Only at higher densities one eventually observes a (weak) sign change of the effective crystal field correction at the lowest border of the parameter region considered ($\Delta_{CF}^d \sim -0.5$).

These results demonstrate the essential role played by the density of the d manifold for determining the final DMFT results on different basis-sets, at least for the important aspect of the Fermi level properties. The starting value of n_d will decide if, *given a correct ab-initio estimate* of the interaction parameters of the multi-orbital

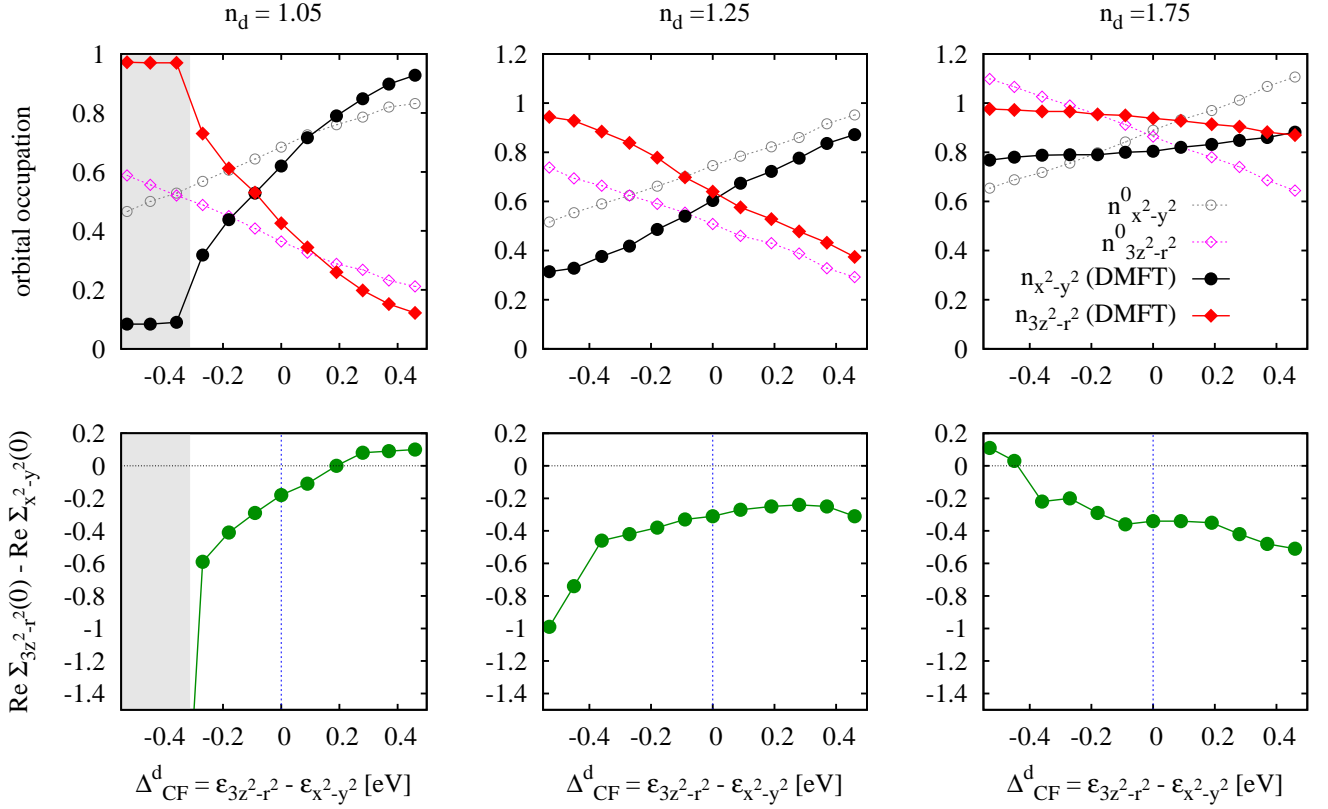


FIG. 8. Upper row: Orbital occupations of the two orbitals of the d -only model with $U' = 4\text{eV}$, $J = 0.75\text{eV}$ ($U = 5.5\text{eV}$), $\beta = 100\text{eV}^{-1}$ for different filling $n_d = 1.05, 1.25, 1.75$ as a function of the initial crystal field splitting Δ_{CF}^d . The DMFT data (solid symbols) are compared with the corresponding non-interacting results (empty symbols). Note that a filling of $n_d = 1.75$ roughly corresponds to the filling of the two d -orbitals in the dp models considered in the previous sections. Lower row: Difference of the real part of the DMFT self-energies for the two orbitals extrapolated at $\omega_n \rightarrow 0$ (solid symbols) as a function of the initial crystal field splitting Δ_{CF}^d for the corresponding set of data.

Hubbard Hamiltonian, the physics of the interacting system will be *driven* by the (original) crystal field, or rather by the Hund's rule tendency for equally occupied orbitals. Therefore, it will be *a priori* quite hard to reconcile DMFT calculations performed on different basis-sets, without considering the corresponding occupation of the *correlated* manifolds.

From the perspective of actual material calculations, the strong dependence of the final LDA+DMFT results for the Ni-based heterostructures can be put in a rather general framework. In fact, the quarter-filling physics particularly favors the crystal field-dominated physics, since the Hund's exchange is weaker in a system with one electron (on average). Hence, if the dp hybridization can drive the system away from this regime (as is the dp model considered here with an average filling of $n_d \sim 1.75$), the Hund's exchange will easily prevail over the crystal field effects. The same interpretation can likely explain, why the results of LDA+DMFT calculations for the Fe-based superconductors do not display, in most cases, such crucial dependence on the basis-set considered. There, the five orbitals of the Fe $3d$ manifold are

characterized by a small value of the *overall* orbital energy splitting $\sim 0.2\text{eV}$ (in comparison to the typical values of the order of 1eV observed in many transition metal oxides). This corresponds to a situation of *five* partially filled ($n_d \sim 6^{61}$) correlated orbitals all very close energetically to the Fermi level, i.e. one of the most favorable playground for strong Hund's exchange processes. Hence, this case is well inside one of the two regimes, and moderate differences in the orbital occupation of the d manifold in different basis-sets will *not* result in a qualitative discrepancy between different LDA+DMFT calculations, with the possible exception of the regimes closest to the Mott transitions^{62,64,65}.

V. CONCLUSIONS

We have thoroughly compared two models for transition metal oxides: a d -only model containing two effective d -orbitals and a dp model made of two d - and two p -orbitals. On the single-particle level without Coulomb interaction, the two models show the same low-energy

physics and band-structure. However if the Coulomb interaction is taken into account by means of DMFT, this is not the case any more.

The main reason for this discrepancy is the number of d -electrons. In the d -only model there is on average one d -electron per site. For the dp model on the other hand, the bands are filled with altogether 5 electrons per site: Without hybridization the two p -orbitals at lower energy would be completely filled, and the d -orbitals in the vicinity of the Fermi level would have the same filling (one electron per site) as for the d -only model. The d -orbitals hybridize however with the p -orbitals, and, hence, there is some admixture between the orbitals leading to a larger filling (~ 1.7) of the d -orbitals for the dp model.

This different filling has dramatic consequences for the correlated solution of the two models. For the d -only model the Coulomb interaction enhances the initial crystal field splitting, leading to a situation with one d -electron in the lowest-lying d -orbital. Depending on the original crystal field (e.g., if $\Delta_{CF}^d > 0$), this can be the $x^2 - y^2$ -orbital, which hence dominates the low energy physics and Fermi surface topology. This kind of physics can result in a very similar $x^2 - y^2$ -shaped Fermi surface in Ni-based heterostructures as in cuprates.

In contrast, in the dp model the Hund's exchange favors a more even occupation of the two orbitals because the d manifold is much closer to half-filling ($n_d = 2$). The initial crystal field splitting is therefore reduced and the local moment enhanced^{58,66,67}. However, if J is low enough this tendency can be weakened recovering qualitatively the results of the d -only model (see Fig. 7).

Vice versa, we have also verified that the d -only model displays a similar Hund's physics as that of the dp model, if we enhance the d -electron occupation towards the one of the dp model. Let us stress that, while an influence of the filling of the correlated manifold on the DMFT results is not surprising in itself, our study identifies its crucial importance for the description of the low-energy physics. In particular, two important aspects have been determined: (i) the rapidity with which qualitative robust trends found in the d -only basis-sets can be reversed by slightly varying the density from the "nominal" one (e.g. from $n_d = 1$ in our case), (ii) the similarity of the interaction effects in different basis-sets observed in presence of a correspondingly similar occupation of the correlated orbitals.

The findings of our model study have important conse-

quences for the analysis and the interpretation of realistic LDA+DMFT calculations for several transition metal oxides and related correlated materials: The physical results for d -only LDA+DMFT calculations can indeed dramatically differ from calculations which also include the Oxygen p -orbitals. In fact, since the additional p -orbitals lead to a different d -filling, this can determine the aforementioned dramatically different low-energy DMFT physics. Eventually, in the case of contradicting DMFT prediction, experiments (such as, e.g., ARPES or X-ray absorption spectroscopy or orbital reflectometry) will show which of the two theoretical set-ups describes the physical reality better.

Furthermore we should note that, as the dp calculation is generally far away from an integer filling of the interacting d -orbitals, the occurrence of Mott-Hubbard metal-insulator transitions becomes more difficult^{35,36}. Certainly one can expect non-local correlations beyond DMFT³⁷ to be of importance for (quasi) two-dimensional Mott insulators. However, not showing a Mott insulating phase in other specific cases might well be a deficit of the dp calculations or, at least, of the way such dp calculations are performed nowadays, e.g., via the complete neglect of the dp interaction.

Let us emphasize, finally, that in other situations the physics of the d -only and dp calculation can be much more similar. This was e.g. observed in most of the DMFT studies on iron pnictides. In these materials, the presence of a large manifold of partially filled correlated $3d$ -orbitals all close to the Fermi level is a common aspect for both dp and d -only calculations. Hence, in both cases the physics is mostly dominated^{14,62} by Hund's rule forming a large local magnetic moment in a correlated metallic environment.

Acknowledgments

We acknowledge financial support from by the Deutsche Forschungsgemeinschaft (DFG) and the Austrian Science Fund (FWF) through the Research Units FOR 1346 (FWF I597-N16, A. T.) and FOR 1162 (DFG, N. P. and G. S.) and SFB ViCom F41 (K. H.). We thank O.K. Andersen for exchanging opinions and for his detailed comments about our manuscript, and S. Biermann M. Capone, A. Georges, M. Haverkort, J. Kuneš, L. de Medici, and P. Wissgott for fruitful discussions.

¹ J. Hubbard, Proc. Roy. Soc. London A **276**, 238 (1963); M. C. Gutzwiller, Phys. Rev. Lett. **10**, 159 (1963); J. Kanamori, Progr. Theor. Phys. **30**, 275 (1963).

² W. Metzner and D. Vollhardt, Phys. Rev. Lett. **62**, 324 (1989).

³ A. Georges, G. Kotliar, W. Krauth, and M. Rozenberg, Rev. Mod. Phys. **68**, 13 (1996).

⁴ V. I. Anisimov, A. I. Poteryaev, M. A. Korotin, A. O. Anokhin and G. Kotliar, J. Phys. Cond. Matter **9** (1997), 7359; A. I. Lichtenstein, and M. I. Katsnelson, Phys. Rev. B **57**, 6884 (1998); G. Kotliar, S. Y. Savrasov, K. Haule,

- V. S. Oudovenko, O. Parcollet and C. A. Marianetti, *Rev. Mod. Phys.* **78**, 865 (2006); K. Held, *Adv. Phys.* **56**, 829 (2007).
- ⁵ N. F. Mott, *Rev. Mod. Phys.* **40**, 677 (1968); *Metal-Insulator Transitions* (Taylor & Francis, London, 1990); F. Gebhard, *The Mott Metal-Insulator Transition* (Springer, Berlin, 1997).
 - ⁶ K. Held, G. Keller, V. Eyert, D. Vollhardt, and V. I. Anisimov, *Phys. Rev. Lett.* **86** 5345 (2001).
 - ⁷ S. Y. Savrasov, G. Kotliar and E. Abrahams, *Nature* **410** 793 (2001).
 - ⁸ A. I. Lichtenstein, M. I. Katsnelson and G. Kotliar, *Phys. Rev. Lett.* **87** 067205 (2001).
 - ⁹ K. Held, A. K. McMahan and R. T. Scalettar, *Phys. Rev. Lett.* **87** 276404 (2001).
 - ¹⁰ M. Capone, M. Fabrizio, C. Castellani, and E. Tosatti, *Science* **296**, 2364 (2002).
 - ¹¹ K. Byczuk, M. Kollar, K. Held, Y.-F. Yang, I. A. Nekrasov, T. Pruschke, and D. Vollhardt, *Nature Physics* **3**, 168 (2007).
 - ¹² A. Toschi, M. Capone, C. Castellani, and K. Held, *Phys. Rev. Lett.* **102**, 076402 (2009).
 - ¹³ K. Haule, J. H. Shim, and G. Kotliar, *Phys. Rev. Lett.* **100**, 226402 (2008); L. Craco, M. S. Laad, S. Leoni, and H. Rosner, *Phys. Rev. B* **78**, 134511 (2008).
 - ¹⁴ K. Haule and G. Kotliar, *New J. Phys.* **11**, 025021 (2009); P. Hansmann, R. Arita, A. Toschi, S. Sakai, G. Sangiovanni, and K. Held, *Phys. Rev. Lett.* **104**, 197002 (2010); A. Toschi, R. Arita, P. Hansmann, G. Sangiovanni, K. Held, *Phys. Rev. B* **86**, 064411 (2012); N. Lanatá, H. U. R. Strand, G. Giovannetti, B. Hellsing, L. de' Medici, M. Capone, *Phys. Rev. B* **87** 045122 (2013).
 - ¹⁵ A. Valli, G. Sangiovanni, O. Gunnarsson, A. Toschi, and K. Held, *Phys. Rev. Lett.* **104**, 246402 (2010).
 - ¹⁶ M. Potthoff and W. Nolting, *Phys. Rev. B*, **60** 7834 (1999).
 - ¹⁷ S. Okamoto, *Phys. Rev. Lett.* **101**, 116807 (2008).
 - ¹⁸ P. Hansmann, Xiaoping Yang, A. Toschi, G. Khaliullin, O.K. Andersen, and K. Held, *Phys. Rev. Lett.* **103** 016401 (2009).
 - ¹⁹ P. Hansmann, A. Toschi, Xiaoping Yang, O.K. Andersen, K. Held, *Phys. Rev. B*, **82** 235123 (2010).
 - ²⁰ M. Uchida, K. Ishizaka, P. Hansmann, Y. Kaneko, Y. Ishida, X. Yang, R. Kumai, A. Toschi, Y. Onose, R. Arita, K. Held, O. K. Andersen, S. Shin, and Y. Tokura, *Phys. Rev. Lett.* **106**, 027001 (2011); M. Uchida, K. Ishizaka, P. Hansmann, X. Yang, M. Sakano, J. Miyawaki, R. Arita, Y. Kaneko, Y. Takata, M. Oura, A. Toschi, K. Held, A. Chainani, O. K. Andersen, S. Shin, and Y. Tokura, *Phys. Rev. B* **84**, 241109 (2011).
 - ²¹ J. Chaloupka and G. Khaliullin, *Phys. Rev. Lett.* **100**, 016404 (2008).
 - ²² We note that such an enhanced crystal field splitting in DMFT has been first observed in realistic calculations for V_2O_3 ²³ as well as in model multi-orbital studies²⁴.
 - ²³ G. Keller, K. Held, V. Eyert, D. Vollhardt, and V. I. Anisimov, *Phys. Rev. B* **70**, 205116 (2004); A. I. Poteryaev, J. M. Tomczak, S. Biermann, A. Georges, A. I. Lichtenstein, A. N. Rubtsov, T. Saha-Dasgupta, and Ole K. Andersen, *Phys. Rev. B* **76**, 085127 (2007).
 - ²⁴ A. I. Poteryaev, M. Ferrero, A. Georges, and O. Parcollet, *Phys. Rev. B* **78**, 045115 (2008).
 - ²⁵ P. Hansmann, PhD Thesis, Vienna University of Technology, Austria (April 2010).
 - ²⁶ G. Wannier, *Dynamics of Band Electrons in Electric and Magnetic Fields*, *Rev. Mod. Phys.*, **34**, 645 (1962); N. Mazari and D. Vanderbilt, *Phys. Rev. B*, **56**, 12847 (1997).
 - ²⁷ O. K. Andersen, *Electronic Structure and Physical Properties of Solids: The Uses of the LMTO method*, Lecture Notes in Physics Springer, New York (2000).
 - ²⁸ For examples of typical Wannier functions in different basis sets, see M. W. Haverkort, M. Zwierzycki and O. K. Andersen, *Phys. Rev. B* **85**, 165113 (2012)
 - ²⁹ J. Kuneš, V. I. Anisimov, S. L. Skornyakov, A. V. Lukoyanov, and D. Vollhardt, *Phys. Rev. Lett.* **99**, 156404 (2007).
 - ³⁰ J. Kuneš, L. Baldassarre, B. Schächner, K. Rabia, C. A. Kuntscher, Dm. M. Korotin, V. I. Anisimov, J. A. McLeod, E. Z. Kurmaev, and A. Moewes, *Phys. Rev. B* **81**, 035122 (2010).
 - ³¹ A. Perucchi, C. Marini, M. Valentini, P. Postorino, R. Sopracase, P. Dore, P. Hansmann, O. Jepsen, G. Sangiovanni, A. Toschi, K. Held, D. Topwal, D. D. Sarma, and S. Lupi, *Phys. Rev. B* **80**, 073101 (2009).
 - ³² J. Kuneš, V. Krápek, N. Parragh, G. Sangiovanni, A. Toschi, and A. V. Kozhevnikov, *Phys. Rev. Lett.* **109**, 117206 (2012).
 - ³³ V. Krápek, P. Noák, J. Kuneš, D. Novoselov, Dm. M. Korotin and V. I. Anisimov, *Phys. Rev. B* **186**, 195104 (2012).
 - ³⁴ M. Aichhorn, L. Pourovskii, V. Vildosola, M. Ferrero, O. Parcollet, T. Miyake, A. Georges, and S. Biermann, *Phys. Rev. B* **80**, 085101 (2009); S. L. Skornyakov, A. V. Efremov, N. A. Skorikov, M. A. Korotin, Yu. A. Izyumov, V. I. Anisimov, A. V. Kozhevnikov, and D. Vollhardt, *Phys. Rev. B* **80**, 092501 (2009); S. L. Skornyakov, A. A. Katanin, and V. I. Anisimov, *Phys. Rev. Lett.* **106**, 047007 (2011); M. Aichhorn, L. Pourovskii, and A. Georges, *Phys. Rev. B* **84**, 054529 (2011).
 - ³⁵ K. Held, <http://online.kitp.ucsb.edu/online/cem02/held> (unpublished).
 - ³⁶ Xin Wang, M. J. Han, Luca de' Medici, Hyowon Park, C. A. Marianetti, and Andrew J. Millis, *Phys. Rev. B* **86**, 19513 (2007).
 - ³⁷ T. Maier *et al.*, *Rev. Mod. Phys.* **77** 1027 (2005); G. Kotliar *et al.*, *Phys. Rev. Lett.* **87** 186401 (2001); A. I. Lichtenstein and M. I. Katsnelson, *Phys. Rev. B* **62** 9283 (R) (2000); A. Toschi, A.A. Katanin, and K. Held, *Phys. Rev. B* **75**, 045118 (2007); A. N. Rubtsov, M. I. Katsnelson, and A.I. Lichtenstein, *Phys. Rev. B* **77**, 033101 (2008); G. Rohringer, *et al.*, *Phys. Rev. B* **88**, 115112 (2013).
 - ³⁸ M.J. Han, Xin Wang, C.A. Marianetti, and A.J. Millis, *Phys. Rev. Lett.* **107** 206804 (2011); *ibid.* **110**, 179904(E) (2013).
 - ³⁹ F. Lechermann, S. Biermann, and A. Georges, *Progress of Theoretical Physics Supplement* **160**, 233 (2005).
 - ⁴⁰ Note: the completely filled t_{2g} -orbitals can affect the broadening of the corresponding high-frequency part of the photoemission spectra, but *not* the low-energy electronic structures close to the Fermi level⁴⁴.
 - ⁴¹ P. Löwdin, *J. Chem. Phys.* **19**, 1396 (1951)
 - ⁴² See also O.K. Andersen, "NMTOs and their Wannier functions", Chap. 3, p. 26-27 in *Correlated Electrons: From Model to Metals*, Lecture Notes of the Autumn School Correlated Electrons 2012, edited by E. Pavarini, E. Koch, F. Anders and M. Jarrell, Jülich (2012).
 - ⁴³ O.K. Andersen, A.I. Lichtenstein, O. Jepsen, F. Paulsen, *J. Phys. Chem. Solids* **56**, 1573 (1995).

- ⁴⁴ X. Deng, M. Ferrero, J. Mravlje, M. Aichhorn, and A. Georges, Phys. Rev. B **85**, 125137 (2012).
- ⁴⁵ Geometrically, it corresponds to a tetragonal distortion, a compression or elongation along one of the cubic C^4 axes, of the ligand octahedron.
- ⁴⁶ V. I. Anisimov, J. Zaanen and O. K. Andersen, Phys. Rev. B **44** 943 (1991).
- ⁴⁷ M. Karolak, G. Ulm, T. O. Wehling, V. Mazurenko, A. Poteryaev, A. I. Lichtenstein, J. of Electron Spectroscopy and Related Phenomena, **181**,11 (2010).
- ⁴⁸ P. Werner and A. J. Millis, Phys. Rev. B, **74** 155107 (2006).
- ⁴⁹ E. Gull, A. J. Millis, A. I. Lichtenstein, A. N. Rubtsov, M. Troyer, P. Werner, Rev. Mod. Phys. **83**, 2 (2011)
- ⁵⁰ K. Haule, Phys. Rev. B **75**, 155113 (2007).
- ⁵¹ N.Parragh, A. Toschi, K. Held, G. Sangiovanni, Phys. Rev. B, **86** 155158 (2012).
- ⁵² E. Benckiser, M. Haverkort, *et al.* Nat. Materials (2011).
- ⁵³ Note that the sign of the Hartree difference depends also on the value of the Hund's exchange J (see also Ref. 39). However, for plausible values of J , the condition $U > 5J$ is typically fulfilled, and, hence, the sign prefactor in Eq. 8 can be usually assumed as positive.
- ⁵⁴ Note that the trends emerging from our analysis have been tested to be quite stable against the changes of U , in a relatively broad range, while they are more sensible to changes of the Hund's exchange J , as discussed in the text.
- ⁵⁵ We note that the important physics driven by the Hund's exchange processes has attracted a considerable interest in the most recent literature^{56–58}.
- ⁵⁶ P. Werner, E. Gull, M. Troyer, and A. J. Millis, Phys. Rev. Lett. **101**, 166405 (2008).
- ⁵⁷ A. Georges, L. de' Medici, and J. Mravlje, Annual Review of Condensed Matter Physics **4**, 137 (2013).
- ⁵⁸ L. de' Medici, Phys. Rev. B **83**, 205112 (2011) L. de' Medici, J. Mravlje, and A. Georges, Phys. Rev. Lett. **107**, 256401 (2011).
- ⁵⁹ For example from constrained cRPA or even for cRPA locally unscreened calculations⁶⁰.
- ⁶⁰ Y. Nomura, M. Kaltak, K. Nakamura, C. Taranto, S. Sakai, A. Toschi, R. Arita, K. Held, G. Kresse, and M. Imada, Phys. Rev. B **86**, 085117, (2012).
- ⁶¹ See, e.g., the LDA+DMFT systematic study of Fe3d occupation in⁶². We note, though, that higher occupation values have been recently reported in⁶³.
- ⁶² Z.P. Yin, K. Haule and G. Kotliar, Nat. Mat. **10**, 932 (2011).
- ⁶³ T. Schickling, F. Gebhard1, J. Bünemann, L. Boeri, O. K. Andersen, and W. Weber, Phys. Rev. Lett. **108**, 036406 (2012).
- ⁶⁴ L. de' Medici, G. Giovannetti, and M. Capone, arXiv:1212.3999.
- ⁶⁵ F. Hardy, *et al.*, Phys. Rev. Lett. **111**, 027002 (2013)
- ⁶⁶ P. Werner and A. J. Millis, Phys. Rev. Lett. **99**, 126405 (2007); M. Sentef, J. Kuneš, P. Werner, and A. P. Kampf, Phys. Rev. B **80**, 155116 (2009).
- ⁶⁷ J. C. Budich, B. Trauzettel and G. Sangiovanni, Phys. Rev. B **87**, 235104 (2013).